

## Bent-crystal monochromators for high-energy synchrotron radiation

Hitoshi Yamaoka,<sup>a\*</sup> Tetsuro Mochizuki,<sup>b</sup> Yoshiharu Sakurai<sup>a</sup> and Hiroshi Kawata<sup>c</sup>

<sup>a</sup>The Institute of Physical and Chemical Research (RIKEN), Mikazuki, Sayo, Hyogo 679-5143, Japan, <sup>b</sup>The Japan Synchrotron Radiation Research Institute (JASRI), Mikazuki, Sayo, Hyogo 679-5198, Japan, and <sup>c</sup>High Energy Accelerator Research Organization (KEK), 1-1 Oho, Tsukuba 305-0801, Japan. E-mail: yamaoka@spring8.or.jp

(Received 4 August 1997; accepted 2 December 1997)

Two kinds of monochromators covering the energy ranges 100–150 keV and  $\sim$ 300 keV have been designed for inelastic (Compton) scattering experiments at the elliptical multipole wiggler beamline, BL08W, of SPring-8. Finite-element analyses using ANSYS for bent crystals indicate that thermal problems are not serious for the 300 keV monochromator, while an energy spread of about  $10^{-3}$  for the 100–150 keV monochromator is possible in the centre of the crystal. Detailed calculations of X-ray interaction with the silicon crystal were performed. The results show that Compton scattering is a dominant process and deposits about 100 W continuously.

**Keywords:** monochromators; bent crystals; high energy; Compton scattering.

### 1. Introduction

At SPring-8, two kinds of monochromators are installed at the wiggler beamline BL08W for inelastic (Compton) scattering experiments (Sakurai *et al.*, 1995; Yamaoka *et al.*, 1996). One monochromator covers the energy range from 100 to 150 keV for high-resolution Compton scattering experiments and the other operates at  $\sim$ 300 keV for magnetic Compton scattering experiments. Both monochromators are designed for a single-crystal arrangement. The 100–150 keV monochromator is doubly bent (Kawata *et al.*, 1989, 1998). A symmetric Johann-type Si 400 reflection will be used in the first phase and in the future an asymmetrically cut crystal will be used. The crystal surface is set horizontally. It is bent to obtain a vertically focused beam at the position given by  $q/p = 1$ , where  $p$  and  $q$  are distances from source to crystal and crystal to focal point, respectively. In the sagittal direction, the crystal is bent with a fixed radius ( $q/p = 1/3$ ). An asymmetric Johann type is employed for the 300 keV monochromator. The Si 771 reflection will be used with an asymmetry angle of about  $1^\circ$  to make the crystal length smaller and the focal point forward. The crystal surface is vertical. The crystal is set to focus a vertically diverged beam. We use Bragg geometry because we can obtain an efficiently focused beam for both monochromators compared with Laue geometry. The focal spot sizes are expected to be about  $0.5 \times 0.5$  mm for a 100–150 keV beam and  $1$  mm (width)  $\times$   $3$  mm (height) for a 300 keV beam, from ray-tracing calculations (Sakurai *et al.*, 1995). Four-point crystal benders are used for both kinds of monochromators

for simplicity. Here we report the design of the monochromators, crystal bender, and results of some calculations concerning the heat-load analyses and radiation problem.

### 2. Radiation and heat-load problem

#### 2.1. Microprocess and radiation problem

The radiation problem is serious in this beamline because the wiggler source provides relatively high-energy X-rays. Fig. 1(a) shows an example of the calculated power distribution on a silicon crystal at a Bragg angle of  $3.2^\circ$  as a function of the crystal thickness. We use the OEHL code (Tong *et al.*, 1992, 1995). AP, HP, Cb, Ct, Rb and Rt are absorbed power, pure heat power, Compton backscattered power, Compton transmitted power, Rayleigh backscattered power and Rayleigh transmitted power, respectively. Compton scattering is dominant and deposits about 100 W into the other components such as the vacuum vessel, bender, stages *etc.* continuously. A water-cooled system surrounds the crystal. For the 300 keV monochromator, the primary crystal shield consists of a water-cooled rectangular Cu tube aligned around the crystal and crystal holder parallel to the beam axis. As the secondary shield a water-cooled Cu skin of 5 mm thickness is adjusted inside the vacuum vessel. A third shield is 20 mm-thick lead which covers the outside of the vacuum vessel. The local lead shielding means that the white-beam hutch lead shielding may be thinner. For the 100–150 keV monochromator, the

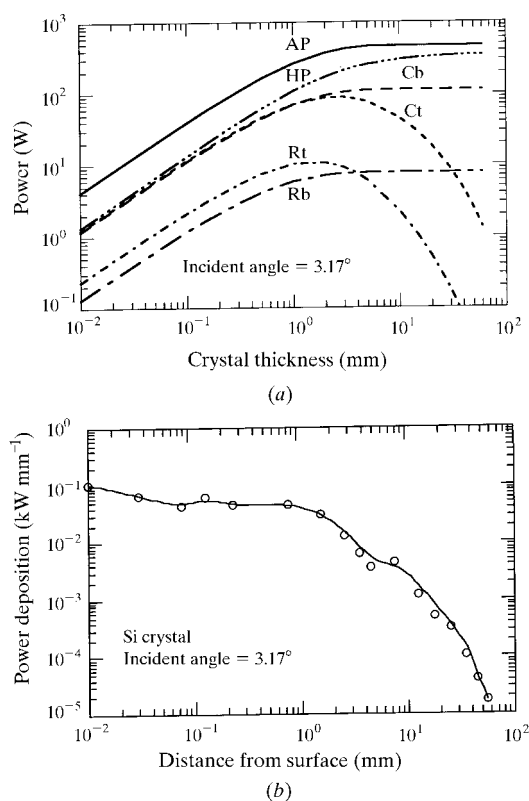


**Figure 1**

(a) Power distribution of a silicon crystal at a glancing angle of  $3.2^\circ$  as a function of crystal thickness at BL08W of SPring-8. AP, HP, Cb, Ct, Rb and Rt are absorbed power, pure heat power, Compton backscattered power, Compton transmitted power, Rayleigh backscattered power and Rayleigh transmitted power, respectively ( $AP = HP + Cb + Ct + Rb + Rt$ ). (b) Power deposition rate ( $\text{kW mm}^{-2}$ ) as a function of the distance from the crystal surface.

primary shield is a water-cooled Cu plate just above the crystal to protect it from the scattered X-rays. The other shields are similar to those of the 300 keV monochromator. Fig. 1(b) shows the energy deposition as a function of the distance from the crystal surface. The change in the power deposition rate is small until a distance of about 1 mm. It decreases at larger distances.

## 2.2. Heat load on bent crystals

In this beamline the insertion device is an elliptical multipole wiggler (EMPW) with parameters  $l = 12$  cm,  $K_y = 11.2$ ,  $K_x = 0-1.1$ ,  $N = 37$ ,  $L = 4.5$  m and a total maximum power of 18 kW for  $K_x = 0$  (Marechal *et al.*, 1995). When a 36 mm-thick graphite filter and 20 mm-thick Al filter are inserted before the optics, the incident power of the monochromator is reduced to about 800 W for the maximum power input. For the 100–150 keV monochromator, precise slot channels are bored to obtain a high heat-transfer coefficient just below the Cu holder surface where the 3 mm-thick crystal will be clamped through a liquid In–Ga layer. The slotted channel is 1 mm in width and 9 mm in height, as shown in Fig. 2(a). The pure absorbed power by the silicon crystal is calculated by *OEHL* code to be about 400 W for an incident power of 800 W. A heat-transfer coefficient of  $0.01 \text{ W m}^{-2} \text{ K}^{-1}$  is assumed and a force of 20–30 N is applied to the crystal. The crystal holder has a fixed radius of curvature in the sagittal direction. As an example, the results of finite-element analyses are shown in Fig. 3(a). For the 100–150 keV monochromator, the best performance of the bent crystal, which has an energy resolution of  $\sim 10^{-3}$ , is possible only in the centre of the crystal. Other calculations were also made. We studied the holder thickness effect by changing it from 20 mm to 30 mm, but the difference was small. The holder material was changed from Cu to Si; the result showed that the deformation becomes larger due to lower heat conductivity of Si compared with Cu. The precise slot channels give a better performance compared with the hole channels.

For the 300 keV monochromator, an additional filter of 10 mm-thick Al is inserted and results in an incident power of 464 W. The model and results of the finite-element analyses for the bent

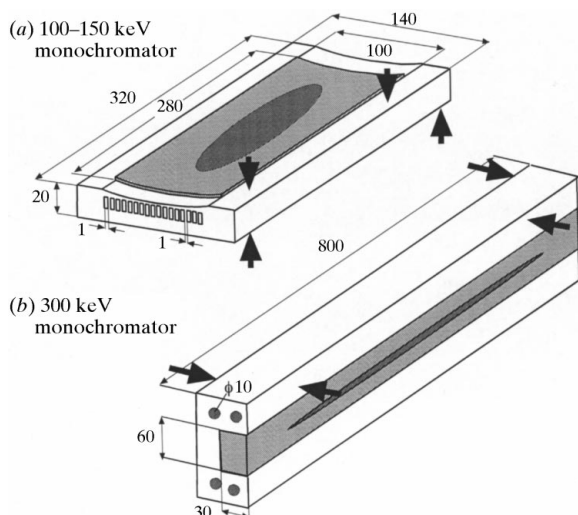


**Figure 2**

Model of the crystal and the crystal holder used in the calculation for (a) the 100–150 keV monochromator and (b) the 300 keV monochromator. The crystal surfaces are set to be horizontal for the 100–150 keV monochromator and vertical for the 300 keV monochromator. Units: mm.

crystal are shown in Fig. 2(b) and Fig. 3(b). For the 300 keV monochromator, the crystal block is indirectly water-cooled from both sides through a thin In–Ga layer. Heat-transfer coefficients of  $0.008 \text{ W mm}^{-2} \text{ K}^{-1}$  between water and Cu and  $0.036 \text{ W mm}^{-2} \text{ K}^{-1}$  between In–Ga and Si, a fluid velocity of  $1.06 \text{ m s}^{-1}$  (total flow rate of  $20 \text{ l min}^{-1}$ ) and irradiated area of  $534 \times 4.4 \text{ mm}$  are assumed. The results indicate that for the 300 keV monochromator the thermal problem is not serious. Here we note that, even for a temperature change along the beam direction of only a few degrees, the deformation of the bent crystal is quite large, especially at the ends of the crystal. By cutting the end parts of the reflected beam after the crystal with slits, the best performance will be given without losing the flux.

## 3. Monochromators

### 3.1. Crystal bender and bent crystal

The bender design we propose is based on a four-point bending system operated at either end of the crystal or the crystal holder using two stepper motors, each in a sine-bar configuration. As shown in Fig. 4, the crystal bending is achieved through the twist of two shafts *A* which are connected to the other bar *B* vertically. A small linear motion of bar *B* provides a twist of shaft *A* and the crystal is bent. Both shafts can be controlled independently. This bender has some advantages. First, we can apply the bending force through a linear motion of bar *B* and it is easily realized. Second, the bender is not affected by the temperature change in the shafts. A small change in the incident angle produces a large change in the reflection energy because the incidence angle is very small in these monochromators. If the shafts *A* of the bender are connected to the crystal holder vertically, a small temperature rise of the columns produces a significant effect on the change in the incident angle. It is noted

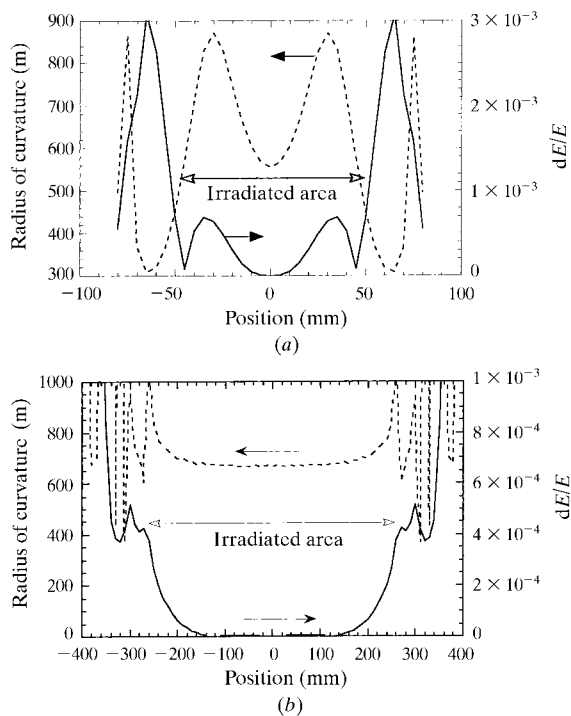


**Figure 3**

Results of the ANSYS calculation for (a) the 100–150 keV monochromator crystal and (b) the 300 keV monochromator crystal.

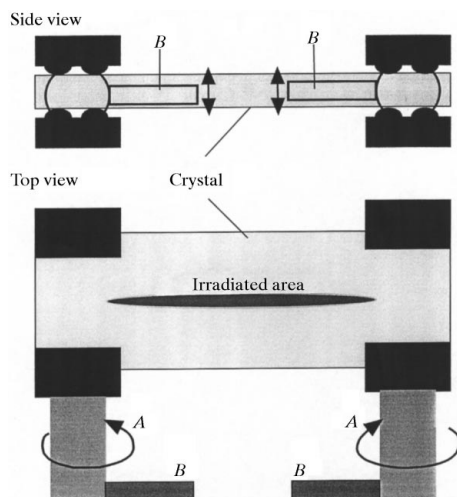


**Figure 4**

Concept of the SPring-8 BL08 monochromator bender. The shaft *A* is twisted by linear motion of the bar *B* to realize four-point bending. The same system is used for both kinds of monochromators.

that scattered X-rays heat up the bender components. In our system the temperature change in the columns *A* does not affect the incident angle of the crystal.

The effect on angle resolution of a bent crystal was studied by using analytical formulae and simulation with Takagi-Taupin equations (Yamaoka *et al.*, 1998). The results show that at  $\sim 100$  keV the dynamical effect is dominant for a bent radius of curvature of about 1000 m, while at  $\sim 300$  keV the kinematical effect becomes dominant at almost any time for the bent crystal. The energy spreads of these monochromators are unnecessarily narrow even though the crystals are bent, as indicated by the above calculations. A mosaic crystal, such as an annealed or polished one, would be one way to obtain a much more integral intensity. A study of mosaic crystals was performed, and a polished crystal will be used (Yamaoka *et al.*, 1997).

### 3.2. 100–150 keV monochromator

For the 100–150 keV monochromator, a symmetric Johann-type Si 400 crystal will be mounted on the cylindrical water-cooled Cu holder through a liquid In–Ga interface. The holder will be bent with the crystal by the bender mentioned above so as to obtain a focus given by  $q/p = 1/3$ . The crystal will be cooled indirectly through the Cu holder through which precise slot water-cooled channels will be bored, and the holder will be nickel plated. Access to the chamber and the above system will be *via* the side flange through which the main Bragg rotation will be introduced into the chamber. This side flange will be able to be manually withdrawn horizontally along a rail system for ease of assembly and maintenance. Bragg rotation will be performed outside the vacuum chamber and coupled to the mounting flange through a hollow-bore rotary shaft. The vacuum vessel will be mounted on a translation stage which can be manually moved up and down *via* a linked jacking system. Just above the crystal, a

water-cooled Cu plate will be placed to protect the crystal surface from the radiation. The pipes for the water-cooling circuit will be introduced into the vacuum chamber through the central bore of the main Bragg-angle rotation shaft as usual. Due to limited space, the 300 keV beam from the 300 keV monochromator will pass through the chamber.

### 3.3. 300 keV monochromator

For the 300 keV monochromator, an asymmetric Johann-type Si 771 reflection will be employed with an asymmetry angle of about  $1^\circ$ . The Si 771 crystal surface will be cut from an Si ingot crystal grown in the [001] direction. The crystal size will be about  $800 \times 60 \times 30$  mm. We may also use a thin crystal so both 100–150 keV and 300 keV beams may be employed simultaneously. Essentially the crystal bending mechanism will be similar to that of the 100–150 keV monochromator except that the reflecting face will be vertical as opposed to horizontal. The crystal will be bent to focus the beam in the horizontal plane. The system within the vacuum vessel will consist of the Bragg rotation, the crystal up and down translation, and horizontal translation. The whole system will be on the thick base plate which will act as a kinematic mount within the vessel. All motions will be decoupled from the vacuum vessel. For protection from the direct beam irradiation to the crystal, two apertures, including Pb and water-cooled Cu, will be set before and after the crystal.

The authors are grateful to Dr T. Ishikawa for some suggestions about the monochromator design and encouragement, and Mr J. Tanase of TOYAMA Co. Ltd for the suggestion of the crystal bender. We also thank the staff of IHI, Mr H. Saito, Mr M. Marushita, Mr A. Tetsuka and Mr S. Mandai, who constructed these monochromators.

### References

- Kawata, H., Miyahara, T., Yamamoto, S., Shioya, T., Kitamura, H., Sato, S., Asaoka, S., Kanaya, N., Iida, A., Mikuni, A., Sato, M., Iwazumi, T., Kitajima, Y. & Ando, M. (1989). *Rev. Sci. Instrum.* **60**, 1885–1888.
- Kawata, H., Sato, M., Higashi, Y. & Yamaoka, H. (1998). *J. Synchrotron Rad.* **5**, 673–675.
- Marechal, X. M., Tanaka, T. & Kitamura, H. (1995). *Rev. Sci. Instrum.* **66**, 1937–1939.
- Sakurai, Y., Yamaoka, H., Kimura, H., Marechal, X. M., Ohtomo, K., Mochizuki, T., Ishikawa, T., Kitamura, H., Kashiwara, Y., Harami, T., Tanaka, Y., Kawata, H., Shiotani, N. & Sakai, N. (1995). *Rev. Sci. Instrum.* **66**, 1774–1776.
- Tong, X. M., Yamaoka, H., Nagasawa, H. & Watanabe, T. (1995). *J. Appl. Phys.* **78**, 2288–2297.
- Tong, X. M., Yamaoka, H. & Sakurai, Y. (1992). *Proc. Soc. Photo-Opt. Instrum. Eng.* **1739**, 514–521.
- Yamaoka, H., Goto, S., Kohmura, Y., Uruga, T. & Ito, M. (1997). *Jpn. J. Appl. Phys.* **36**, 2792–2799.
- Yamaoka, H., Ohtomo, K. & Ishikawa, T. (1998). *J. Synchrotron Rad.* **5**, 687–689.
- Yamaoka, H., Sakurai, Y., Mochizuki, T., Ohtomo, K. & Kawata, H. (1996). *SPring-8 Annual Report 1995*, pp. 195–196. JASRI, Kamigori, Ako-gun, Hyogo 678–12, Japan.